AD_____

AWARD NUBMER: W81XWH-06-1-0197

TITLE: DRF as a Cholesterol Dependent Regulator of Src in Prostate Cancer

PRINCIPAL INVESTIGATOR: Michael R. Freeman, Ph.D.

CONTRACTING ORGANIZATION: Children's Hospital Boston
Boston, MA 02115

REPORT DATE: October 2009

TYPE OF REPORT: Final

PREPARED FOR: U.S. Army Medical Research and Materiel Command
Fort Detrick, Maryland 21702-5012

REPORT DOCUMENTATION PAGE

Form Approved
OMB No. 0704-0188

1. REPORT DATE *(DD-MM-YYYY)*	**2. REPORT TYPE**	**3. DATES COVERED** *(From - To)*
1 October 2009	Final	15 DEC 2005 - 14 SEP 2009

4. TITLE AND SUBTITLE

DRF as a Cholesterol Dependent Regulator of Src in Prostate Cancer

5a. CONTRACT NUMBER

5b. GRANT NUMBER
W81XWH-06-1-0197

5c. PROGRAM ELEMENT NUMBER

6. AUTHOR(S)
Michael R. Freeman, Ph.D.

E-Mail: michael.freeman@childrens.harvard.edu

5d. PROJECT NUMBER

5e. TASK NUMBER

5f. WORK UNIT NUMBER

7. PERFORMING ORGANIZATION NAME(S) AND ADDRESS(ES)

Children's Hospital Boston
Boston, MA 02115

8. PERFORMING ORGANIZATION REPORT NUMBER

9. SPONSORING / MONITORING AGENCY NAME(S) AND ADDRESS(ES)
U.S. Army Medical Research and Materiel Command
Fort Detrick, Maryland 21702-5012

10. SPONSOR/MONITOR'S ACRONYM(S)

11. SPONSOR/MONITOR'S REPORT NUMBER(S)

12. DISTRIBUTION / AVAILABILITY STATEMENT
Approved for Public Release; Distribution Unlimited

13. SUPPLEMENTARY NOTES

14. ABSTRACT

This project focuses on the novel finding from our group that the diaphanous-related formin protein DRF3 is a signaling molecule positioned downstream from the EGF receptor that intersects with the sine kinase Src in prostate cancer cells. Formins are effectors of small Rho-family GTPases like and provide a direct link between activated membrane receptors and the actin cytoskeleton. They also regulated by a large number of other activators including Src homology 3 (SH3)-containing adaptor proteins and Src family kinases, and can therefore serve as signal integrating platforms inside cell. Evidence was presented in the original proposal that the EGFR˜Drf3˜ Src signaling circuit appears to traverse cholesterol-rich "lipid raft" membranes in prostate cancer cells. Lipid rafts are choleterol- and sphingolipid-enriched membrane microdomains that serve as signal transduction platforms sequestering and excluding signaling proteins and by harboring pre-formed multi-protein complexes. have hypothesized in this project, and in our published work in this area, that cholesterol accumulation in prostate cancer cells may promote oncogenesis by altering the nature of—and/or the of—signals that flow through lipid raft microdomains. Several new lines of evidence consistent this hypothesis have been produced in year 2 and are described and summarized in this report.

15. SUBJECT TERMS
Drf3, cholesterol, Src, prostate cancer, EGFR

16. SECURITY CLASSIFICATION OF:			**17. LIMITATION OF ABSTRACT**	**18. NUMBER OF PAGES**	**19a. NAME OF RESPONSIBLE PERSON**
a. REPORT	**b. ABSTRACT**	**c. THIS PAGE**			USAMRMC
U	U	U	UU	18	**19b. TELEPHONE NUMBER** *(include area code)*

Table of Contents

FINAL REPORT:
DRF3 as a Cholesterol-dependent Regulator of Src in Prostate Cancer
Michael R. Freeman, PhD, Principal Investigator
Grant number: A81XWH-06-1-0197

This project focuseD on the novel finding from our group that the diaphanous-related formin protein, DRF3, is a signaling molecule positioned downstream from the EGF receptor that intersects with the tyrosine kinase Src in prostate cancer cells. Formins are effectors of small Rho-family GTPases, like CDC42, which provide a direct link between activated membrane receptors and the actin cytoskeleton. They are also regulated by a large number of other activators including Src homology 3 (SH3)-containing adaptor proteins and Src family kinases, and can therefore serve as signal integrating platforms inside the cell. Evidence was presented in the original proposal that the EGFR→DRF3→Src signaling circuit appears to traverse cholesterol-rich “lipid raft” membranes in prostate cancer cells. Lipid rafts are cholesterol- and sphingolipid-enriched membrane microdomains that serve as signal transduction platforms by sequestering and excluding signaling proteins and by harboring pre-formed multi-protein complexes. We have hypothesized in this project, and in our published work in this area, that cholesterol accumulation in prostate cancer cells may promote oncogenesis by altering the nature of—and/or the types of—signals that flow through lipid raft microdomains.

Summary of the project conclusions. We have verified the original hypothesis that DRF3 lies downstream from EGFR and upstream of Src in prostate cancer cells. Notably, ***we have identified a novel function for this protein***, as described below. Our findings suggest that DRF3 sits within a signaling node that regulates the transition from the "mesenchymal" phenotype to the "amoeboid" phenotype, and that this signaling mechanism intersects with the EGFR signaling web. Our results analyzing the DRF3 coding locus in human prostate cancer specimens indicate that a high level of chromosomal loss occurs with disease progression at this locus, suggesting that DRF3 plays a role in formation of metastases in humans. ***This is the first link between DRF3 and human cancer at any organ site.*** In February 2009, we submitted a new R01 proposal to the NIH to continue to study the relationship between DRF3 and prostate cancer metastases. In revised form, this proposal received a 3 percentile (top 3%) score.

Task 1. Determine the biological consequences of increasing and lowering cellular DRF3 levels by overexpression or gene silencing experiments in prostate cancer cells.

In studies published in 2009 in *Cancer Research*, we identified DRF3 as a mediator of non-apoptotic plasma membrane blebbing and “oncosome” formation. This is the major finding from the study and we believe it to be highly significant. Oncosomes are recently described microvesicles shed from tumor cells that relay signaling information, *including entire protein complexes*, across cell boundaries. This novel mechanism was recently identified in glioblas-

toma (Al-Nedawi et al., 2008). Our paper is the first to describe this phenomenon in prostate cancer cells.

Inducible formation of non-apoptotic blebs in prostate cancer cells. In experiments where DU145 human PCa cells were stimulated with EGF, we noted extensive membrane blebbing (Fig. 1), which occurred immediately (~5 min) following growth factor treatment and persisted for 24 h. Newly formed blebs were predominantly 0.5-5 µm in diameter and could be labeled with the ganglioside probe cholera toxin B subunit (CTxB; Fig. 1A), a membrane-directed yellow fluorescent protein (pMEM-YFP) (14) (Fig. 1B) or the plasma membrane glycoprotein probe wheat germ agglutinin (not shown). Sporadic bleb formation was also observed in vehicle-treated cells. Blebbing did not coincide with increased rates of cell death (Fig. 1D), indicating that these structures are non-apoptotic membrane blebs described in other cell types (Fackler and Grosse, 2008) but not to our knowledge in prostatic cells. Similar rapid blebbing was evoked from the PC-3 human PCa cell line in response to EGF (Fig. 1A).

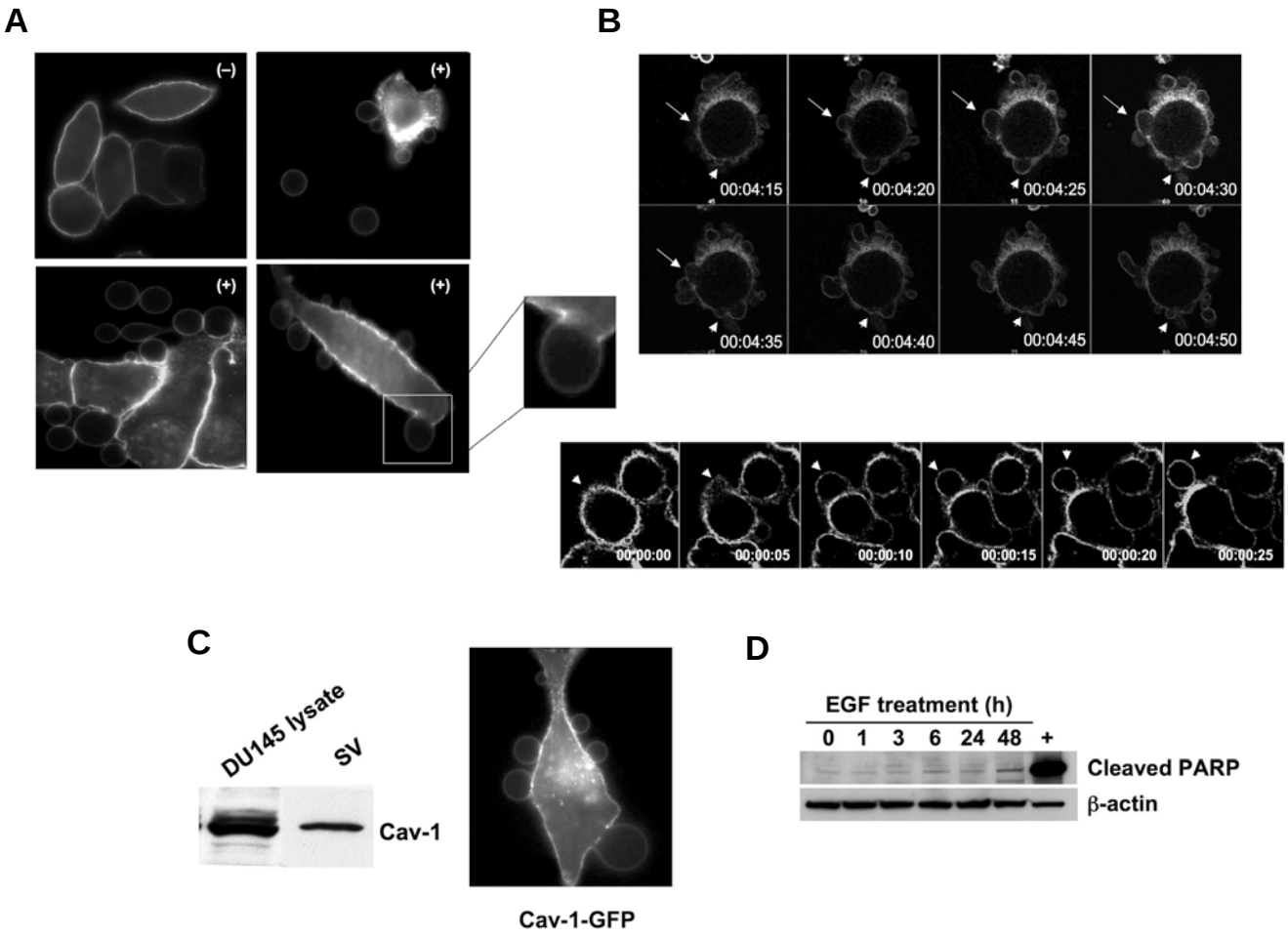

Figure 1: **EGF induces formation of non-apoptotic membrane blebs. (A)** Membrane staining with 0.5 µg/ml FITC-CTxB for 5 min, after 3 h treatment with: (-) vehicle or (+) EGF (50 ng/ml), and imaged by confocal microscopy (63X). All panels show DU145 cells, except the panel at upper right, which shows a PC-3 cell and vesicles

shed (SV) into the medium. The inset shows a single, attached bleb at higher power. **(B)** Frames (5 sec interval) from Movies 1 and 2 acquired by real time confocal microscopy of DU145 cells expressing membrane-targeted pMEM-YFP, and treated with EGF. Panel B shows two examples (differently shaped arrows) of bleb dynamics. **(C)** Lysates from whole cells and SV contain endogenous Cav-1, consistent with localization of a Cav-1-GFP fusion to membrane blebs. **(D)** EGF does not induce apoptosis under these experimental conditions, as shown by an assay for cleaved PARP.

Live confocal imaging of DU145 cells expressing pMEM-YFP and treated with EGF showed blebs emerging rapidly as protrusions, which were sometimes retracted (Fig. 1B). Blebs were also completely extruded from the cell body and released into the medium (Fig. 1A, 1C). Isolation of shed vesicles (SV) by collection of media and ultracentrifugation indicated that they contained the membrane protein caveolin-1 (Cav-1; Fig. 1D), a PCa serum biomarker and an indicator of advanced disease (Tajir et al., 2001). Consistent with this observation, blebs could also be decorated with Cav-1-GFP (Fig. 1D). An in vitro wounding assay showed that rates of bleb formation correlated with increased cell migration (Fig. 2A). The increase in rates of blebbing in response to EGF was completely suppressed by the EGFR inhibitor gefitinib (Fig. 2B i).

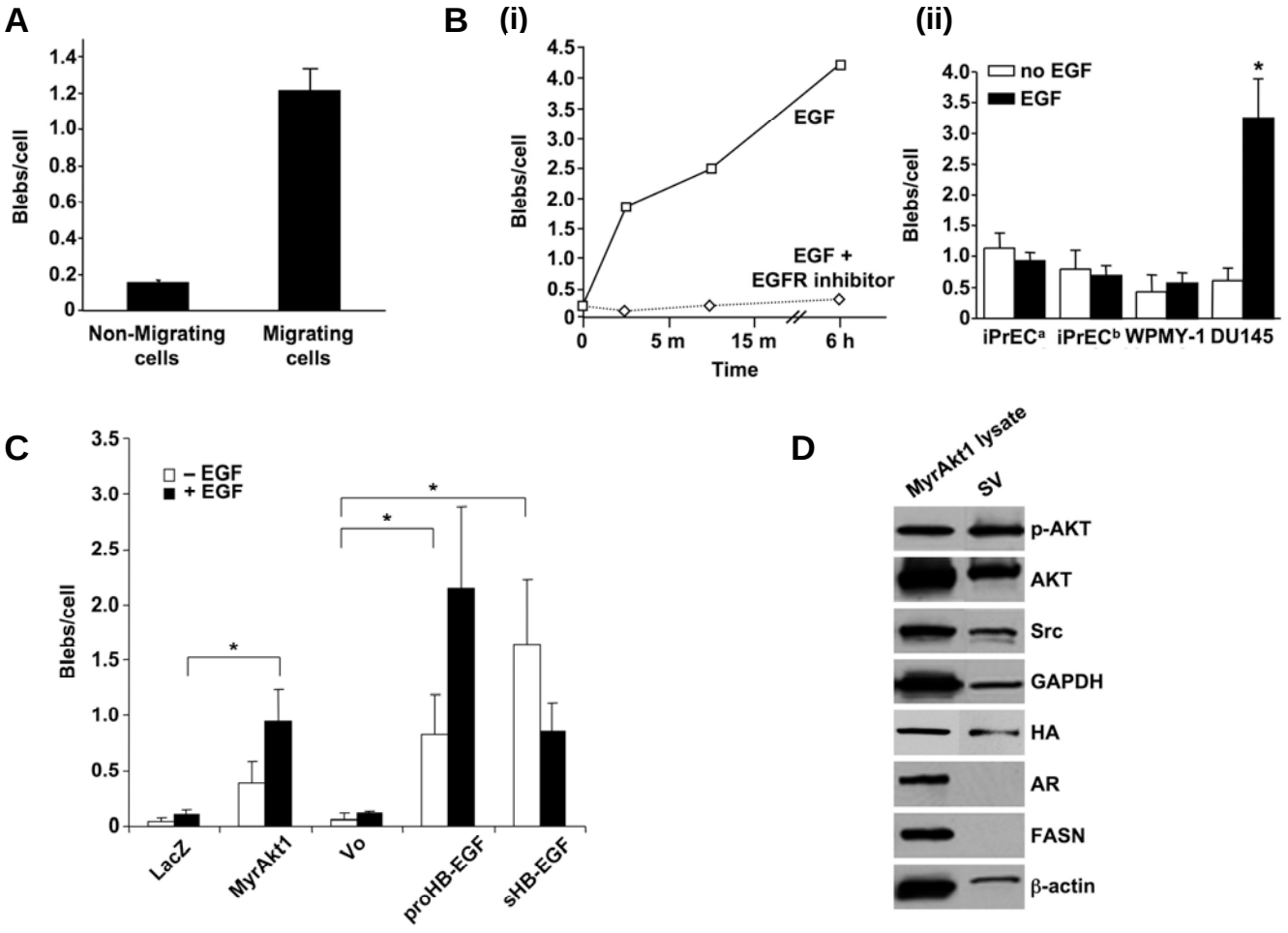

Figure 2: **Blebbing is associated with cell migration, activation of signaling and results in production of shed vesicles that contain membrane proteins. (A)** Bleb formation in DU145 cells treated with EGF (50 ng/ml,

12 h) in a wound healing assay. **(B) (i)** Bleb formation in DU145 cells treated with EGF or EGF plus gefitinib (ZD1839) (10 μM). **(ii)** Bleb formation in prostate normal epithelial (iPrEC) and stromal (WPMY-1) cells, in comparison with DU145, with and without EGF. iPrEC[a] were kept in PrEGM medium, which is serum-free but contains EGF, while iPrEC[b] were transferred to serum-free RPMI 12 h before treatment. **(C)** Bleb formation in LNCaP cells stably engineered to express MyrAkt1, pro-HB-EGF, or soluble (constitutively secreted) sHB-EGF. LacZ (irrelevant gene) and Vo (vector only) are negative controls. **(D)** Protein from whole cell lysates and SV from EGF-treated LNCaP/MyrAkt1 cells were blotted with the indicated Abs.

We observed spontaneous blebbing in LNCaP PCa cells, however basal rates of bleb formation were lower in LNCaP than in DU145, a more aggressive cell line**.** To determine whether blebbing would increase in response to activation of oncogenic signaling, we assessed the extent of bleb formation in LNCaP cells stably expressing the potent membrane-directed oncoprotein MyrAkt1, the membrane-associated precursor form of the EGFR ligand HB-EGF (proHB-EGF), or a soluble form of HB-EGF (sHB-EGF) that is released constitutively into the medium (Adam et al., 2002). Blebbing was significantly increased in LNCaP cells expressing either proHB-EGF or sHB-EGF in the absence of exogenous EGF (Fig. 2C). Addition of EGF further increased blebbing in MyrAkt1- and proHB-EGF-expressing cells (Fig. 2C). Consistent with their sustained export of high levels of sHB-EGF, EGF did not have a further stimulatory effect on LNCaP/sHB-EGF cells. Bleb formation in normal prostate epithelial and stromal cells was modest and unresponsive to EGF (Fig. 2B ii), however in this case blebbing was not a reflection of EGFR level or sensitivity to ligand (not shown).

Bleb secretions contain numerous signal transduction proteins. Because secreted vesicles (SV) contained Cav-1, we hypothesized they might contain other signaling proteins as cargo. SV from LNCaP/MyrAkt1 and LNCaP cells transfected with an irrelevant gene (LacZ) were isolated by collection of medium, followed by ultracentrifugation. SV contained the membrane-associated proteins Akt and Src (Fig. 2D), however we did not detect the largely nuclear androgen receptor (AR) and the predominantly cytosolic enzyme fatty acid synthase (FASN), both of which are expressed at high levels in LNCaP cells. We detected HA-tagged MyrAkt1 in SV from LNCaP/MyrAkt1 cells (Fig. 2D), however endogenous Akt1 was also present in LNCaP/LacZ cells SV (not shown).

To identify protein cargo in SV in an unbiased manner, LNCaP/LacZ and LNCaP/MyrAkt1 SV protein was fractionated by SDS-PAGE. Two prominent zones containing the most abundant proteins ran at ~80 and ~30 kDa (not shown). These zones were excised and analyzed by tandem mass spectrometry (LC-MS/MS). Each protein was identified from at least two unique peptides with an ion score of no less than 40 ($p<0.01$). SV proteins were sorted according to their MOWSE scores and semi-quantified using spectral counting. Numerous signaling proteins involved in cell metabolism, mRNA processing and cell growth and motility were identified (Fig. 3A). The majority of SV proteins were present in both sublines, although as shown, there were some quantitative differences (only proteins with less than 15 spectral counts in at least one sample are shown). This result suggests the possibility of changes in SV protein composition with alterations in signal transduction (e.g., upregulation Akt signaling in LNCaP/MyrAkt1 cells). Multiple proteins of potential relevance to cancer progression were found, including: (1) the cancer-cell-specific isoform of pyruvate kinase M2 (PKM2), a phosphotyrosine-binding protein that promotes increased cell growth and tumor development; (2) programmed

cell death 6 interacting protein (PDCD6IP), also known as Alix, recently shown to inhibit apoptosis; (3) poly(A)-binding protein 1, which associates with paxillin and promotes cell migration; and (4) hnRNP-K, a multifunctional regulator of transcription and translation induced by extracellular growth promoting signals that enhance cancer cell proliferation.

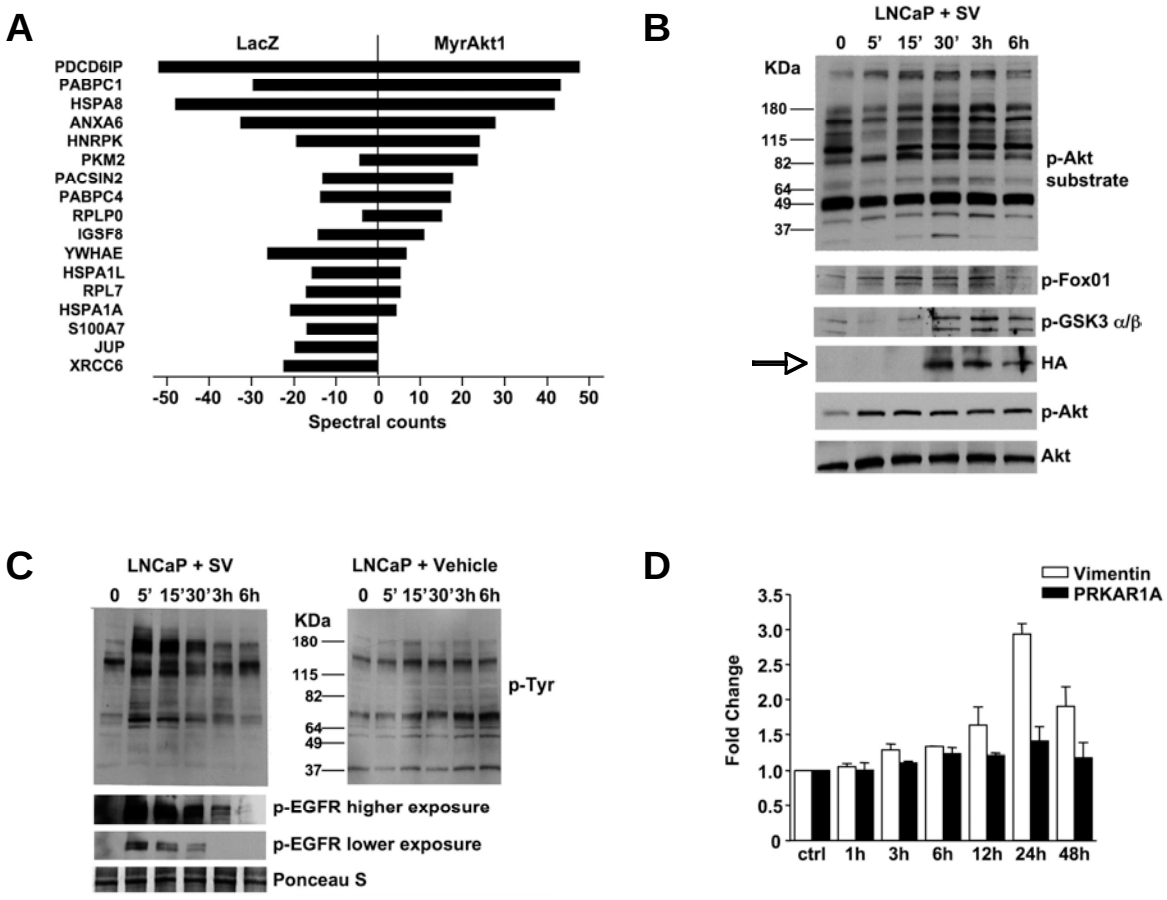

Figure 3: **Shed vesicles exhibit oncosome activity. (A)** Proteins identified by tandem mass spectrometry in bleb material and quantified using spectral counting. PDCD6IP (Programmed Cell Death 6 Interacting Protein), PABPC1 (Poly(A) Binding Protein, Cytoplasmic 1), HSPA8 (Heat Shock 70kDa Protein 8), ANXA6 (Annexin A 6), hnRNP-K (Heterogeneous Nuclear Ribonucleoprotein K, PKM2 (Pyruvate Kinase M2), PACSIN2 (Protein Kinase C and Casein Kinase Substrate in Neurons 2), PABPC4 (Poly(A) Binding Protein, Cytoplasmic 4), RPLPO (Ribosomal Protein Large P0-like Protein), IGSF8 (Immunoglobulin Superfamily, member 8), YWHAE (Tyrosine 3-monooxygenase/tryptophan 5-monooxygenase Activation Protein, Epsilon Polypeptide), HSPA1L (Heat Shock 70kDa Protein 1-Like), RPL7 (Ribosomal Protein L7), HSPA1A (Heat Shock 70kDa protein 1A), S100A7 (S100 calcium binding protein A7), JUP (Junction Plakoglobin), XRCC6 (X-ray Repair Complementing defective repair in Chinese hamster cells 6). **(B)** LNCaP/LacZ cells were exposed to SV obtained from EGF-treated LNCaP/MyrAkt1 cells. Blotting of whole cell lysates is shown. **(C)** LNCaP/LacZ exposed to 20 µg of SV or vehicle from EGF-treated LNCaP/MyrAkt1 cells and assessed for p-Tyr (upper panels). The lower panels show the results of blotting with p-EGFR antibody (p-Tyr^{1068}). **(D)** WPMY-1 cells were exposed to LNCaP/MyrAkt1 derived SV for the indicated times. Vimentin mRNA was quantified by qRT-PCR in recipient cells, and normalized using GAPDH. An irrelevant gene, PRKAR1A, was used as control.

Mass spectrometry data were analyzed using the MetaCore data mining tool (http://www.genego.com) in order to determine whether bleb/SV cargo could be organized into coherent networks and linked to one or more biological processes. Three statistically significant associations with GeneGo ontology pathway or biological process models, all related to mRNA translation, were identified using SV proteins from LNCaP/LacZ cells (Table 1). Interestingly, a much greater number of significant associations was detected using SV cargo from LNCaP/MyrAk1 cells (9 such associations with LNCaP/Akt1 cells vs. 3 seen with LNCaP/LacZ cells), including links to cytoskeletal rearrangement, cell cycle progression, inflammation, DNA damage, cell adhesion and mRNA translation. These data suggest the possibility that the vesicles originating from plasma membrane blebs might be able to relay signals across cell boundaries in a manner similar to recently described glioblastoma-derived oncosomes (Al-Nedawi et al., 2008).

Pathway models	LacZ (-log P)	MyrAkt1(-log P)
Translation: Elongation: Termination	3.9	(n/s)
Cytoskeleton: Regulation of cytoskeleton rearrangement	(n/s)	4.7
Cell cycle: Meiosis	(n/s)	5.9
Cytoskeleton: Cytoplasm microtubules	(n/s)	(n/s)
Inflammation: IL-6 signaling	(n/s)	4.1
DNA damage: Check point	(n/s)	4.1
Inflammation: TREMI signaling	(n/s)	3.9
Cell cycle: GI-S	(n/s)	3.6
Cell adhesion: Cell junctions	(n/s)	3.6
Transduction: Translation initiation	4.5	(n/s)
Biological process models	LacZ (-log P)	MyrAkt1(-log P)
Glycolysis and gluconeogenesis	(n/s)	(n/s)
Vitamin K metabolism	(n/s)	(n/s)
Transcription: Role of heterochromatin protein(HPI) family in transcriptional silencing	(n/s)	1.5
Cell cycle: Role of 14-3-3 proteins in cell cycle regulation	(n/s)	5.7
Translation: Regulation of translation initiation	1.6	(n/s)
Cytoskeleton remodeling: Neurofilament	(n/s)	(n/s)
Glycolysis and gluconeogenesis	(n/s)	(n/s)
Transcription: Role of AP in regulation of cellular metabolism	(n/s)	(n/s)
Cell cycle: Spindle assembly and chromosome separation	(n/s)	(n/s)
Development: Role of CDKS in neuronal development	(n/s)	(n/s)

n/s: not significant

Table 1. Proteins identified by mass spectrometry were analyzed by MetaCore software (GeneGo Inc.) using two algorithms in which the output is either an intracellular signaling pathway or a biological process. Significance was defined as $p<0.05$.

Horizontal signaling. Because analysis of LNCaP SV cargo suggested that the bleb-derived material might possess bioactivities described for oncosomes, we asked whether LNCaP/MyrAkt1 SV are capable of altering signal transduction in recipient cells in a horizontal fashion. SV were isolated from LNCaP/MyrAkt1 cells and recovered material was quantified by

determining protein content. Recipient LacZ cells exposed to SV from LNCaP/MyrAkt1 cells showed a time-dependent activation of the Akt pathway (Fig. 3B), as assessed using a consensus Akt phosphorylated substrate antibody. Consistent with this, levels of active Akt1 (p-S473) and its phosphorylated targets GSK3α/β (p-S21/9) and FoxO1 (p-S256) increased in a time dependent manner. In these experiments, HA-tagged MyrAkt1 was transferred to recipient cells (Fig. 3B, arrow). This finding demonstrates that vesicles shed by LNCaP/MyrAkt1 cells possess activities associated with oncosomes. They also show that an oncoprotein (MyrAkt1) can be transferred across cell boundaries with SV as a vehicle. Consistent with these data, LNCaP/MyrAkt1 SV also evoked robust p-Tyr signaling and EGFR pathway activation in recipient cells (Fig. 3C). SV material also elicited increased levels of vimentin mRNA in WPMY-1 prostate stromal cells (Fig. 3D), suggesting that the vesicles are capable of evoking a stromal reaction.

The actin nucleating protein DRF3/Dia2 inhibits bleb formation. Non-apoptotic membrane blebbing arises from membrane deformations resulting from actomyosin contraction and has been linked to amoeboid cell motility and matrix invasion (Gadea et al., 2007). These findings imply that actin remodeling may affect oncosome formation. To test this idea, we focused on DRF3 (Diaphanous Related Formin 3), the human homolog of the mouse actin nucleating protein Drf3/mDia2. DRF3 is encoded on chromosome 13q, which contains a region of genomic instability in PCa (Dong et al., 2001). An inhibitor of Drf3 was recently reported to induce non-apoptotic blebbing (Eisenmann et al., 2007), suggesting the possibility that DRF3 may oppose blebbing.

DRF3 knockdown by RNA interference (RNAi), using a pool of four siRNA oligos targeted to DRF3, dramatically increased bleb formation in the presence of EGF (Fig. 4A-C), a result that implicates cytoskeletal dynamics in the blebbing process. To determine whether SV derived from cells in which DRF3 had been knocked-down would affect cell behavior in recipient cells, we performed proliferation and migration assays using DU145 cells exposed to SV derived from DU145 cells in which DRF3 expression was reduced by RNAi. Cell proliferation and migration were increased in recipient cells exposed to SV isolated from DU145 cells treated with DRF3 siRNA, at a level quantitatively comparable to that elicited in donor cells by activation of EGFR alone (Fig. 4D).

Frequent chromosomal deletions at the DIAPH3 locus in metastatic prostate cancer. The above findings suggest that DRF3 is capable of inhibiting the blebbing/amoeboid phenotype. To determine the potential relevance of these observations to human PCa, we evaluated the human DRF3 locus (DIAPH3) for chromosomal alterations using 100K SNP arrays, profiling 12 primary PCa tumors and 27 metastatic tumors. A total of 19 (49%) of these tumors exhibited deletions at the DIAPH3 locus (Fig. 5A), much higher than the overall 20% rate of deletion across the genome. Although all of these tumors, including the primaries, were sufficiently enriched to observe copy-number changes elsewhere in the genome, at the DIAPH3 locus deletions were observed more frequently among metastases (18 out of 27 (67%)) than primaries (1 out of 12 (8.3%)) (2-sided Fisher's exact test, $p = 0.001$). In a different cohort of patient samples, fluorescence in situ hybridization (FISH), an alternative method, was used to assess the DIAPH3 locus for chromosomal alterations. FISH results indicated chromosomal loss of DIAPH3 in 7 out of 35 (20%) primaries, and 9 out of 14 (64%) metastases (Fig. 5B), confirming a significantly higher frequency of deletions in aggressive disease in compari-

son with primary tumors (2-sided Fisher's exact test, p = 0.006). DIAPH3 deletion was not detected in benign tissues.

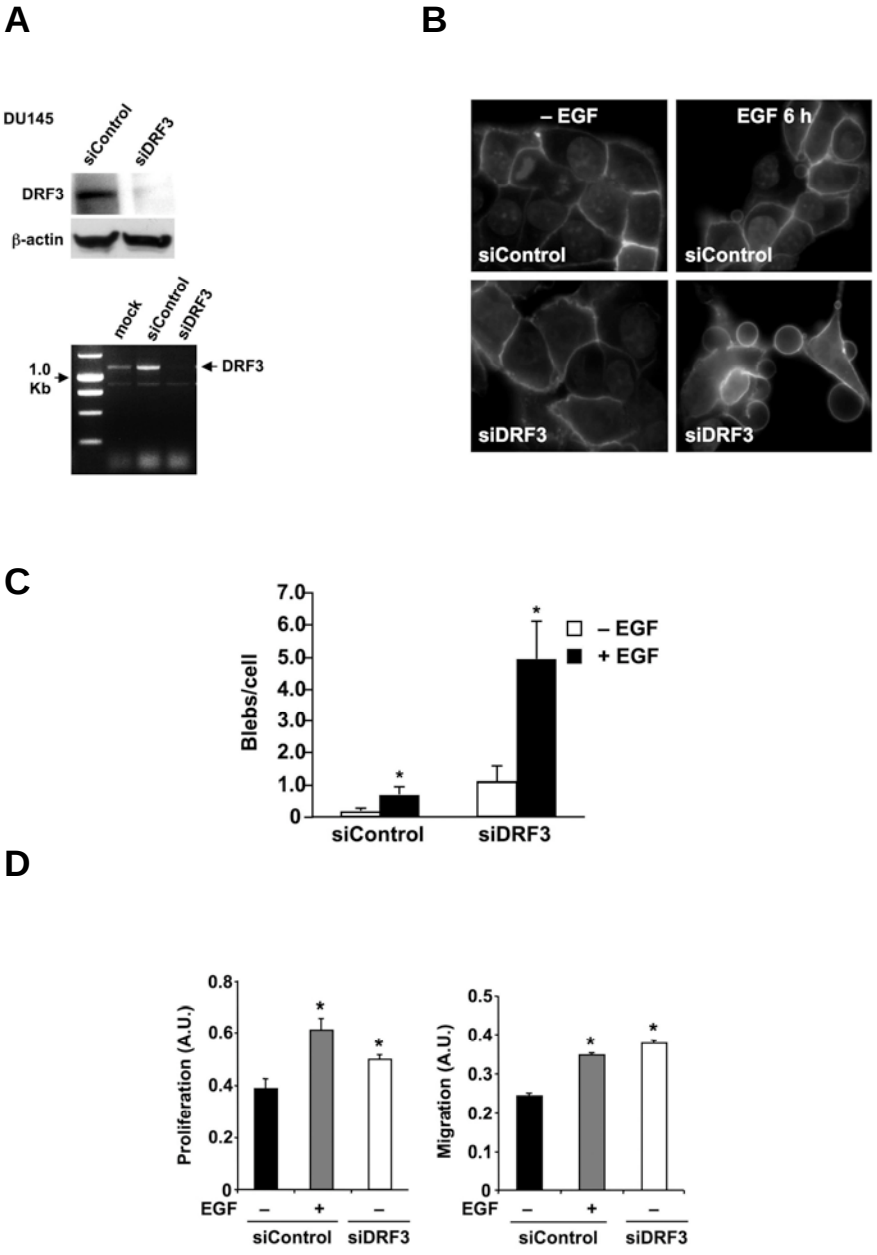

Figure 4: **DRF3 knockdown by RNA interference results in oncosome secretion. (A)** Verification of DIAPH3 gene silencing by siDRF3 in DU145 cells by western blot (upper panel) and RT-PCR (lower panel). Control non-targeting siRNA was a negative control. **(B)** FITC-CTxB staining of DU145 cells showing blebbing in siDRF3-transfected or siRNA control cells, with or without EGF (3 h) (right panel). **(C)** Quantitative analysis of bleb formation in DU145 cells treated with siRNA for DRF3 or control siRNA, +/- EGF. **(D)** Proliferation assay (left panel) and migration assay (right panel) in DU145 cells treated with SV prepared from DU145 cells treated with siRNA control oligos, +/- EGF, or with DRF3-targeted oligos. *p<0.05.

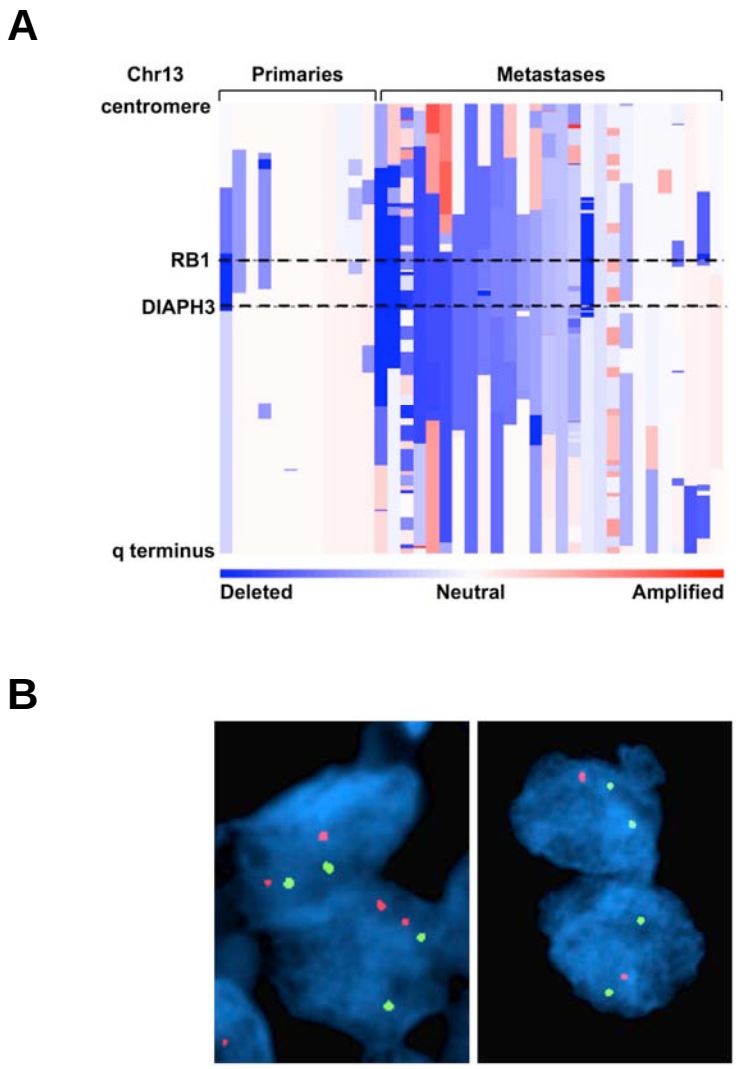

***Figure 5*: Genomic profiling of primary and metastatic prostate cancer at the DIAPH3 locus. (A)** Amplifications (red) and deletions (blue), determined by segmentation analysis of normalized signal intensities from 100K SNP arrays (see Methods), are displayed for 39 prostate cancers (x-axis; primaries and metastases are designated along the top) for the q arm of chromosome 13 (chromosomal positions indicated along the y-axis include the centromere, q-terminus, and RB1 loci). **(B)** DIAPH3 fluorescent in situ hybridization was performed by dual color FISH on PCa tissues. The FISH image on the left shows both red signals (DIAPH3 locus on chr13q21.2) and green signals (a stable region on chr21q22.12) in representative nuclei indicating no deletion of DIAPH3 in tumor cells. The FISH image on the right shows one red signal (DIAPH3 locus on chr13q21.2) and two green signals (a stable region on chr21q22.12) in representative nuclei. Loss of the second red signal is consistent with deletion at DIAPH3. Original magnification of FISH images, 60 X objective.

The above results were published in 2009 in *Cancer Research*. In the *Cancer Res.* paper, we describe the production of non-apoptotic membrane blebs in human PCa cells in response to activation of oncogenic signaling (EGFR and Akt activation). Formation of these dynamic structures correlates with cell migration and, when shed from tumor cells, they elicit bio-

logical responses in recipient cells in a manner that resembles--but is mechanistically distinct from--paracrine signaling. We conclude that the microvesicles we have studied here are functionally equivalent to the bioactive oncosomes recently described as products of aggressive glioblastoma cells (Al-Nedawi et al., 2008). We also identify the actin nucleating protein DRF3 as an endogenous inhibitor of oncosome formation. Analysis of primary and metastatic prostate tumors using high density SNP arrays and FISH resulted in a highly significant association between chromosomal loss at the DRF3 (DIAPH3) locus and metastatic disease. To our knowledge, this is the first study that describes oncosome formation by PCa cells, the first to link formation of SV with non-apoptotic blebbing, and the first to provide evidence for involvement of the formin DRF3 in metastases in any tumor system. Oncosome activity was demonstrated in two unrelated PCa cell line backgrounds, LNCaP and DU145, and similar membrane blebbing was evoked in PC-3 cells in response to EGF, suggesting that this is a general phenomenon. The precise relationship between the surprisingly large (0.5-5μm) SV we have observed here by fluorescence microscopy, using several membrane probes, and the smaller (<0.1-1 μm) secreted vesicles reported by other groups (Cocucci et al., 2009) remains to be determined.

The results of unbiased mass spectrometry studies, analysis of known proteins, and bioinformatics evaluation of SV cargo proteins are consistent with the finding that oncosome formation can result in transfer of membrane-associated protein complexes within the tumor microenvironment. Oncosomes might also be vectors of certain cancer progression markers that are detectable in the circulation. One such marker, Cav-1, identified in our study as oncosome cargo, is a circulating biomarker of metastatic PCa (Tajir et al., 2001, 2008). Our data suggest that oncosome secretion is a mechanism whereby the integral membrane protein Cav-1 obtains access to the extracellular space, where it then becomes available to act at distant sites. Another SV cargo protein identified by mass spectrometry is hnRNP-K, which we recently showed to be a novel Akt binding protein and regulator of AR translation (Mukhopadhyay et al., 2009). mRNA translation was repeatedly identified in the present study using the MetaCore software tool as a biological process that was significantly associated with bleb cargo proteins.

Our data indicate that the actin nucleator DRF3 is capable of inhibiting oncosome formation, since DRF3 knockdown by RNAi increased blebbing in DU145 cells, particularly in the presence of EGF. DRF3 is expressed by LNCaP, DU145 and PC-3 human prostate cell lines (data not shown). Formin homology (FH) proteins mediate cytoskeletal dynamics (9, 35) and, as a group, have been implicated in a wide range of cellular functions, including motility and vesicular trafficking. The formin FHOD1, which exhibits 45% sequence homology to DRF3, was recently implicated in Src-dependent plasma membrane blebbing (Hannemann et al., 2008). Human DRF3 is not well studied, although analyses of the mouse homolog Drf3, and the close mouse paralog, Drf1/mDia1, indicate that DRF3 likely mediates actin filament nucleation and elongation and microtubule stability. A DRF3 interactor, the Diaphanous interacting protein DIP, was recently shown to promote plasma membrane blebbing by acting as a Dia inhibitor (Eisenmann et al., 2007). Non-apoptotic membrane blebs can either dissociate from the cell or be retracted in an actin-dependent manner. Blebbing has been linked to the amoeboid form of cell movement (Yoshida and Soldati et al., 2006) and our data indicate that DRF3 likely plays a role within a critical signaling node that controls the amoeboid phenotype. The finding

that DRF3 silencing in SV donor cells resulted in increased cell proliferation and migration in SV recipient cells provides an important new link between: (1) blebbing and the amoeboid phenotype and (2) the production of vesicles that can propagate signals horizontally in the tumor microenvironment. These experimental data are consistent with our analysis of human prostate tumors, indicating that chromosomal loss at the DRF3 coding region is associated with metastatic disease. Loss of function at the DIAPH3 locus from somatic mutation may lead to alterations in the propensity toward invasion or metastasis. We are currently testing this hypothesis experimentally.

Our results suggest that oncosome transfer between tumor cells, or between tumor and stroma, could play a role in propagation of aggressive behavior within the tumor microenvironment. As pointed out by Al-Nedawi et al. (2008), oncosome exchange is markedly different from paracrine effects induced by soluble ligands. However, this process could result in amplification of paracrine pathways through intercellular sharing of membrane-associated signaling complexes. Although our study focuses on PCa, a similar microvesicular transfer mechanism may operate in other tumor systems.

Task 2. **(i)** Identify the phosphorylation sites on Drf3 that are regulated by EGFR activation and **(ii)** determine the functional consequences of phosphorylation at these sites.

As described in an earlier progress report, we have used mass spectrometry to identify an EGFR-responsive phosphorylation site on DRF3 (S624). We subsequently raised a phosphosite-specific antibody against this epitope and showed that this reagent detects the phosphorylation event. We have shown that the antibody can be used to detect phosphorylation of the *endogenous* protein at this site following EGFR activation. We have also shown that the site is sensitive to the presence of the lipid raft protein, Cav-1, and to depletion of membrane cholesterol by methyl-ß-cyclodextrin.

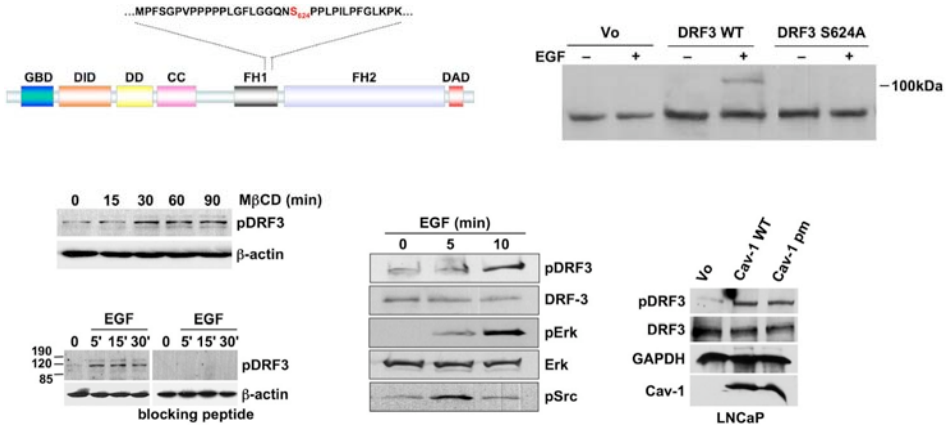

Figure 6. EGF triggers DRF3 phosphorylation. Phosphorylation at serine S624, monitored with a phospho-specific antibody (pDRF3). Specificity is shown by blocking with a peptide corresponding to the S624 neighboring

residues and S624A mutation. Phosphorylation can be elicited by depletion of membrane cholesterol with methyl-b-cyclodextrin, expression of wildtype Cav-1 or a palmitoylation-negative mutant (pm).

Task 3. Identify the binding partners of DRF3 and the physiological contexts in which they act.

We have described in a previous progress report our studies of DRF3 binding to Profilin-1, a G-actin transport protein. Our functional experiments with DRF3 silencing have provided additional evidence that DRF3 is within the EGFR circuit and is biochemically linked to a number of proteins involved in signal transduction and cell-cell interaction. These experiments are still in progress and we have proposed, in our pending R01 grant, to continue these studies. A significant result is our novel finding that DRF3 forms a complex with EGFR that responds to EGFR activation (Figure 6). Formation of this complex could be shown with both endogenous proteins (Figure 6, lower left). Consistent with these data, DRF3 silencing with siRNA results in EGFR activation and activation of downstream EGFR signaling (e.g., note activation of ERK in the figure). These findings are in agreement with our results that DRF3 silencing cooperates with the EGFR in promoting non-apoptotic blebbing of PCa cells (Figure 4).

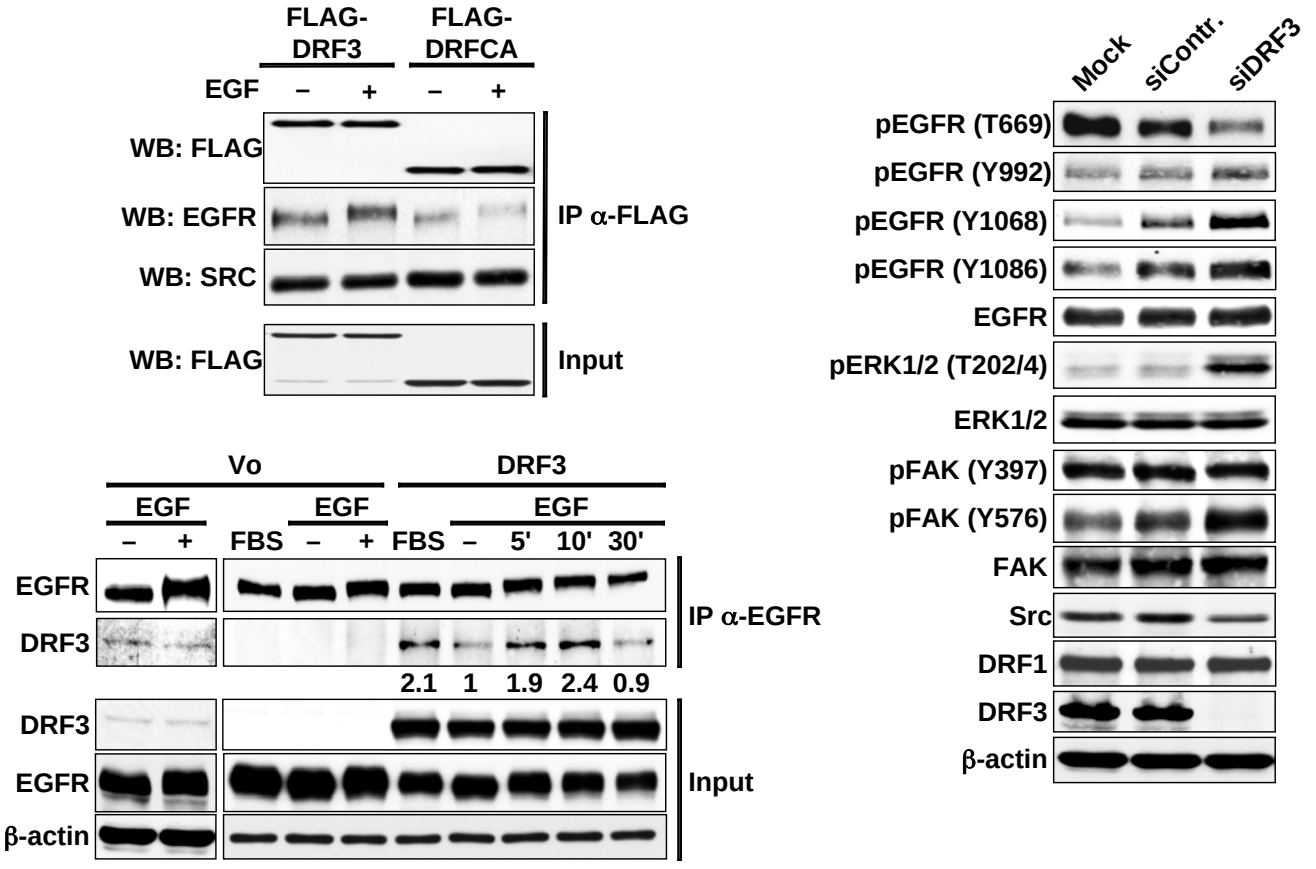

***Figure 6*: DRF3 interacts with EGFR. Left.** DRF3 and constitutively active DRF3 (DRF3CA) bind EGFR. Complex formation increases in response to EGF, peaking at 10 min. **Right.** DRF3-deficient cells show evidence for EGFR (Y1068) and MAP kinase pathway activation.

Task 4. **(i)** Determine whether DRF3 expression functionally suppresses or otherwise alters Src activity or subcellular transit. **(ii)** Determine the subcellular localization and physiological contexts where Src and DRF3 interact and their relevant inteacting partners. **(iii)** Determine whether DRF3 activities are dependent on the presence of Src.

We have shown that DRF3 is upstream of the Src non-receptor tyrosine kinase (Figure 7). To date, we have not detected any reproducible influence of DRF3 on Src. Our present hypothesis is that Src may reside within a DRF3 multi-protein complex that contains EGFR and that Src is a downstream mediator of DRF3. Consistent with this, DRF3 silencing activates the Rho-dependent kinase ROCK (Figure 7), a Src mediator. The question of how DRF3 may be an effector of Src is still open. Significantly, silencing of DRF3 converts DU145 PCa cells from a mesenchymal to an amoeboid phenotype (Figure 7), consistent with our findings on non-apoptotic blebbing, indicating DRF3 likely resides within an important node that controls the transition between these tumor phenotypes. This is now the central hypothesis as these studies go forward.

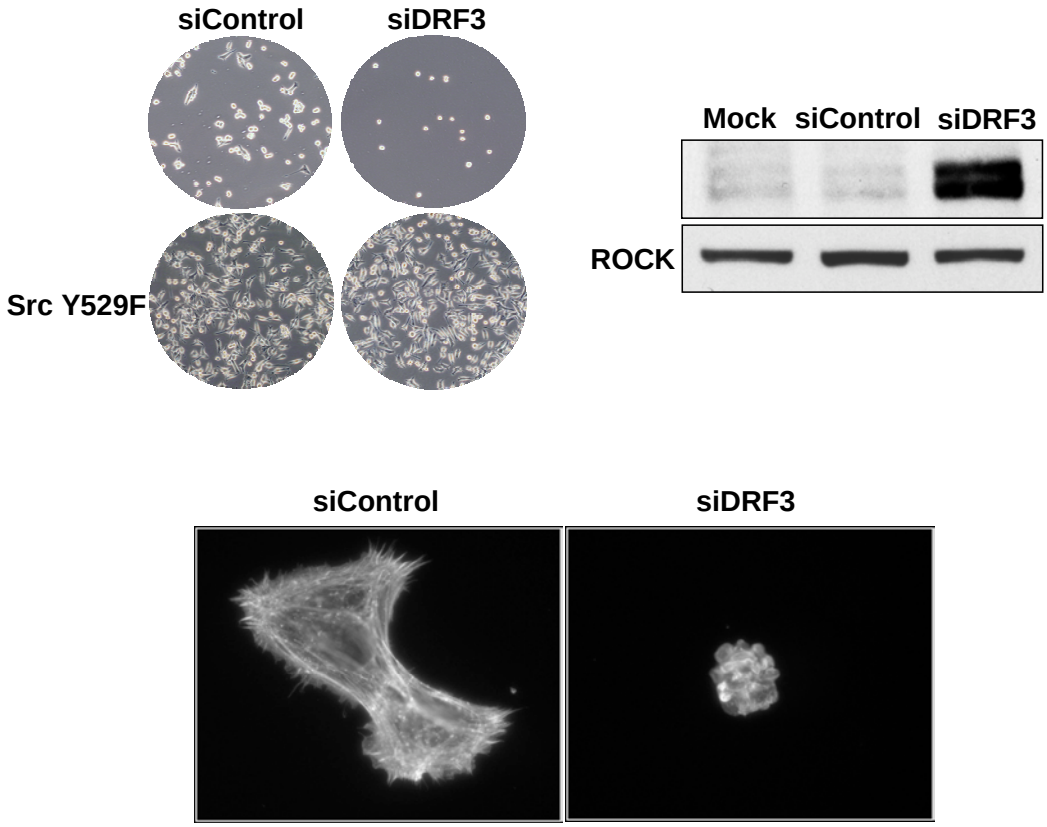

***Figure 7*: DRF3 lies upstream of Src and silencing of DRF3 promotes amoeboid morphology in a 3D-matrix** DU145 cells display a mesenchymal phenotype on collagen I, which transitions to an amoeboid mode of migration in the absence of DRF3. Constitutively active Src (SrcY529F) is able to override this effect, indicating

Src lies downstream of DRF3. ROCK activity is enhanced in the absence of DRF3 as evidenced by strong phosphorylation of the ROCK substrate, MYPT-1

KEY RESEARCH ACCOMPLISHMENTS

- DRF3 controls non-apoptotic blebbing and the amoeboid phenotype in human prostate cancer cells.
- Chromosomal loss at the DRF3 coding locus (DIAPH3) is associated with metastatic prostate cancer.
- DRF3 lies within the EGFR pathway and may be a critical mediator of the amoeboid-mesenchymal transition.

REPORTABLE OUTCOMES

Publications attributable in whole or part to funding from this grant:

Freeman, M.R., Cinar, B., Kim, J., Mukhopadhyay, N.K., Di Vizio, D., Adam, R.M., and Solomon, K.R. (2007) Transit of hormonal and EGF receptor-dependent signals through cholesterol-rich membranes. Steroids. 72:210-217.

Hager, M.H., Solomon, K.R., and **Freeman, M.R.** (2006) The role of cholesterol in prostate cancer. Current Opinion in Clinical Nutrition and Metabolic Care 9:379-385.

Lutchman, M., Solomon, K.R., and **Freeman, M.R**. Cholesterol, cell signaling and prostate cancer. In: Prostate Cancer: Biology, Genetics and the New Therapeutics. Chung, L.W.K., Isaacs, W.B., and Simons, J.W. Second edition. pp. 119-137. Humana Press, Totowa, NJ, 2007.

Yang, W. and **Freeman, M.R.** (2008) Proteomics approaches to the analysis of multiprotein signaling complexes. Proteomics 8:832-851.

Solomon, K.R., and **Freeman, M.R.** (2008) Do the cholesterol-lowering properties of statins affect cancer risk? Trends in Endocrinology and Metabolism 19:113-121.

Di Vizio, D., Solomon, K.R., and **Freeman, M.R.** (2008) Cholesterol and cholesterol-rich membranes in prostate cancer: An update. Tumori 94:633-639.

Qi, M., Liu, Y., **Freeman, M.R**., and Solomon, K.R. (2009) Cholesterol-regulated stress fiber formation. Journal of Cellular Biochemistry 106:1031-1040.

Di Vizio, D., Kim, J., Hager, M.H., Morello, M., Yang, W., Lafargue, C.J., True, L., Rubin, M.A., Adam, R.M., Beroukhim, R., Demichelis, F., and **Freeman, M.R.** (2009) Oncosome formation in prostate cancer: Association with a region of frequent chromosomal deletion in metastatic disease. Cancer Research 69:5601-5609.

NIH grant proposal:

1 R01 CA143777-01. Amoeboid Membrane Dynamics in Prostate Cancer. New R01 grant proposal submitted to the NIH, February 2009. PI: Michael Freeman. The proposal received a 3 percentile score (top 3%) in revised form. Anticipated start date is June 2010.

REFERENCES

Adam RM, Kim J, Lin J, et al. Heparin-binding epidermal growth factor-like growth factor stimulates androgen-independent prostate tumor growth and antagonizes androgen receptor function. Endocrinology 2002; 143: 4599-608.

Al-Nedawi K, Meehan B, Micallef J, et al. Intercellular transfer of the oncogenic receptor EGFRvIII by microvesicles derived from tumour cells. Nat Cell Biol 2008; 10: 619-24.

Cocucci E, Racchetti G, Meldolesi J. Shedding microvesicles: artefacts no more. Trends Cell Biol 2009; 19: 43-51.

Eisenmann KM, Harris ES, Kitchen SM, Holman HA, Higgs HN, Alberts AS. Dia-interacting protein modulates formin-mediated actin assembly at the cell cortex. Curr Biol 2007; 17: 579-91.

Dong JT, Boyd JC, Frierson HF, Jr. Loss of heterozygosity at 13q14 and 13q21 in high grade, high stage prostate cancer. Prostate 2001; 49: 166-71.

Gadea G, de Toledo M, Anguille C, Roux P. Loss of p53 promotes RhoA-ROCK-dependent cell migration and invasion in 3D matrices. J Cell Biol 2007; 178: 23-30.

Fackler OT, Grosse R. Cell motility through plasma membrane blebbing. J Cell Biol 2008; 181: 879-84.

Hannemann S, Madrid R, Stastna J, et al. The diaphanous related formin FHOD1 associates with ROCK1 and promotes Src-dependent plasma membrane blebbing. J Biol Chem 2008.

Mukhopadhyay NK, Kim J, Cinar B, et al. Heterogeneous nuclear ribonucleoprotein K is a novel regulator of androgen receptor translation. Cancer Res 2009; 69: 2210-8.

Tahir SA, Yang G, Ebara S, et al. Secreted caveolin-1 stimulates cell survival/clonal growth and contributes to metastasis in androgen-insensitive prostate cancer. Cancer Res 2001; 61: 3882-5.

Tahir SA, Yang G, Goltsov AA, et al. Tumor cell-secreted caveolin-1 has proangiogenic activities in prostate cancer. Cancer Res 2008; 68: 731-9.

Yoshida K, Soldati T. Dissection of amoeboid movement into two mechanically distinct modes. J Cell Sci 2006; 119: 3833-44.